



A comprehensive ship weather routing system using CMEMS products and A* algorithm

Manel Grifoll ^{a,*}, Clara Borén ^b, Marcella Castells-Sanabra ^b

^a Civil and Environmental Engineering Department, Universitat Politècnica de Catalunya (UPC-BarcelonaTech), Barcelona, 08028, Spain

^b Nautical Science and Engineering Department, Universitat Politècnica de Catalunya (UPC-BarcelonaTech), Barcelona, 08003, Spain

ARTICLE INFO

Keywords:

Weather ship routing
A-star algorithm
CMEMS
Ship emissions
SIMROUTE

ABSTRACT

We describe the implementation of a comprehensive software for Ship Weather Routing referred to as SIMROUTE. The A* pathfinding algorithm is used to optimize the sailing route as a function of the wave action. The aim of the software is to provide a comprehensive, open and easy tool including pre- and post-processing for ship weather routing simulations. The software is constructed considering the Copernicus Marine Environment Monitoring Service (CMEMS) wave predictions systems which are available for free use. The code provides the optimized route and the minimum distance route together with additional modules to compute ship emission and safety on navigation monitoring. SIMROUTE has been tested in several cases using different CMEMS products over short and long distances. The comprehensive structure of the code enables it to be easily modified to include additional ship wave resistance models and the effect of the water currents and winds on navigation. SIMROUTE is also used for academic purposes, providing skills for ship routing optimization in the framework of standards of training, certification and watchkeeping (STCW) for competence-based maritime education and training. Due to the simplicity of its use, SIMROUTE is a good candidate for benchmarking strategies and inter-comparison exercises with advanced methods for ship weather routing. This contribution highlights the technical aspects, code organization and structure behind SIMROUTE, demonstrating its capabilities through examples of route optimization.

1. Introduction

There is a growing concern to reduce emissions in order to mitigate climate change. The environmental impact of transport is significant because it is the major user of energy. Shipping is the prevalent transport mode for overseas freight and is frequently recognized as a sustainable, energy-efficient and relatively environmentally friendly means of transport (Dft, 2004). However, shipping is still a substantial source of greenhouse gas emissions (Chapman, 2007). In this respect, the shipping industry is not exempt from the need to reduce emissions, and several initiatives have been taken by stakeholders and academics to promote sustainable growth (Goldsworthy and Goldsworthy, 2015; Kanellos et al., 2014; Wang et al., 2016; Zakaria et al., 2022; Zis et al., 2014a, 2014b). In the context, global decarbonisation target specific shipping sectors and the academia addresses several pertinent questions on information collection and planning routes (Wu et al., 2021; Zakaria et al., 2022; Zis et al., 2020b). In addition, a major factor of competitiveness in the maritime industry is the minimization of time and fuel consumption

for ship routes. The emerging field of the autonomous ships also shows an increasing interest for optimization tools in the framework of performance management systems that includes analysis and real-time remote monitoring, hindcast/forecast wave conditions and make decision support (e.g. Ruth and Thompson, 2022; Zhao et al., 2022).

From the shipping industry point of view, the minimization of operating costs is a multi-faceted problem, which involves fleet management, vehicle routing problems such as scheduling or ship weather routing, among other strategies. Ship Weather Routing (SWR) is defined as the development of an optimum sailing course and speed for ocean voyages based on nautical charts, the forecasted sea conditions, the captain's experience and the individual characteristics of a ship for a particular route (Simonsen et al., 2015). Academic research has focused on ship routing optimization through pathfinding algorithms (Hinnen-thal and Clauss, 2010; Mannarini et al., 2016; Shin et al., 2020; Simonsen et al., 2015; Szałpczynska and Smierchalski, 2009; Takashima and Mezaoui, 2009; Zhao et al., 2022; Zis et al., 2020a), which take into account meteo-oceanographic forecasts (i.e. wind, waves or

* Corresponding author.

E-mail addresses: manel.grifoll@upc.edu (M. Grifoll), clara.boren@upc.edu (C. Borén), marcella.castells@upc.edu (M. Castells-Sanabra).

<https://doi.org/10.1016/j.oceaneng.2022.111427>

Received 12 October 2021; Received in revised form 17 March 2022; Accepted 25 April 2022

Available online 19 May 2022

0029-8018/© 2022 The Authors. Published by Elsevier Ltd. This is an open access article under the CC BY license (<http://creativecommons.org/licenses/by/4.0/>).

currents predictions). Some of these contributions have been tested through a “proof-of-concept” based on oceanic distances (e.g. Hinnen-thal and Clauss, 2010; Lin et al., 2013; Simonsen et al., 2015), but benchmarking tests have not been found in the literature covering different regional areas. A noticeable effort was made by (Mannarini et al., 2016), using an optimization algorithm based on the graph-search method with time-dependent edge weights in the Mediterranean Sea. In this respect, SIMROUTE presents a flexible structure, permitting all the CMEMS products (which cover all the world’s seas) in a comprehensive design, which creates a fast-executing tool from the user perspective. SIMROUTE may enrich the ship weather routing field of investigation, which has been receiving increasing interest from academics in recent years (see review in Zis et al., 2020a). The code also provides a set of visualization tools for easy and direct inter-comparison of new SWR methods, which may include artificial intelligence and machine learning in the framework of autonomous ship development alternatives (e.g. Kulemann and Tierney, 2020).

The above-mentioned contributions have established an important source of knowledge for seeking efficient ship routes. With a comparable motivation in mind, we present SIMROUTE, an open-source, versatile and computationally efficient software for modelling optimal weather ship routes. SIMROUTE targets one of the aspirations of ship weather routing by minimizing time of navigation and, in consequence fuel consumption and emissions. SIMROUTE has been under active development since 2014 (Grifoll et al., 2018; Grifoll and Martínez de Osés, 2016) and offers modular functionalities including economic assessment, safety in navigation, and emissions estimations oriented to determine the benefit produced by the optimized route, including pre- and post-processing tools for direct and easy use. The Python programming language was chosen as the basis for SIMROUTE due to its flexible, free, and cross-platform-compatible nature. In addition, a MATLAB code version is available that is more oriented to academic purposes. The open-source code (GPL Licenses), together with support materials, is available in [GitHub.com/ManelGrifoll/SIMROUTE](https://github.com/ManelGrifoll/SIMROUTE). Code has been tested using Python 3 and the specific imported modules are included in the headers of the code. This package also provides plotting tools and oriented modules for ship emission or the assessment of safety conditions during navigation. The objective of this contribution is to present the conceptualization, software structure, formulation and the main features of the SIMROUTE, illustrated by examples, as an open-source software for the scientific and teaching community.

The main methodologies used in SWR include the isochrone method (Hagiwara, 1982), dynamic programming (Shao et al., 2012), path-finding algorithms in grid-based approach (Mannarini et al., 2016) and artificial intelligence (Maki et al., 2011) among others (Walther et al., 2016). suggest that grid-based approaches are only suitable for short routes (i.e. coastal shipping) because of its computational efficiency. The improbable smoothness of the solutions is one of the potential drawbacks. However, SIMROUTE uses grid-based approaches A* as a trade-off between accuracy and computational time assuming standard computational resources. Other, conceptual assumptions have been considered in the development of the SIMROUTE software. SIMROUTE assumes that the weather effect increases the total resistance acting in a vessel. Therefore, avoiding bad weather conditions will reduce the sailing time. Also, it means that reducing the sailing time will reduce the fuel consumption and the economic cost per voyage. In consequence, SIMROUTE optimizes the sailing time, taking into account eventual speed reduction due to the waves. In order to evaluate the benefit of the optimization, the minimum distance route is also provided by SIMROUTE.

This paper is organized as follows: after the introduction (Section 1), a SIMROUTE description, methods and accuracy test are presented in Section 2. Section 3 shows test cases also included in the repository. Finally, Section 4 discusses the results and contextualize the work and Section 5 includes concluding remarks, identifying future areas of research.

2. Materials and methods

The software structure consists in a sequential execution of Python scripts. A flow chart to guide SIMROUTE users is shown in Fig. 1, including the folder organization (i.e. *in/*, *out/* and *storeWaves*) and the post-processing tools. Input variables are included in a unique .py file: *params.py*. This set-up file establishes the characteristics of the mesh, period of simulation, wave effect on the navigation model and ship velocity, among other parameters (see Fig. 1 for a short description). The code execution is designed following three steps of .py scripts. The script *get_waves_CMEMS.py* is a pre-processing file that downloads sea surface waves variables in daily files configuration using motuclient from CMEMS repository. Secondly, *make_waves.py* interpolates the wave information into a specific mesh generated as a function of the boundaries and the mesh increment size. Finally, *main.py* executes the optimization algorithm, resulting in two alternatives: an optimized route and a minimum distance route.

2.1. Wave information source

The wave information files are downloaded from the European Union’s Earth observation programme Copernicus. The Copernicus Marine Environment Monitoring Service (CMEMS) provides full, free and open access data and information related to the physical state of the global ocean. Several ocean wave products are provided in the CMEMS catalogue (European Commission, 2021) covering different geographical regions. Fig. 2 shows the regional coverage of the different products excluding the Arctic and Global products also used in SIMROUTE. The *get_waves_CMEMS.py* script downloads the wave files in netcdf format provided by different CMEMS products (forecasting data sets) as a function of a specific flag (*wave_prod*). This script also uses the *param.py* to establish and trim the geographical area of the wave fields. Downloaded wave files are stored in *storeWaves/in* daily format. The products available in the SIMROUTE structure are summarized in Table 1. Motuclient is used to extract and download data through a Python command line. This client enables the handling and transformation of huge volumes of oceanographic data without performance collapse and is available at the GitHub platform.

2.2. Mesh and wave effect on navigation

The computational mesh is established as a function of the grid resolution (*inc* variable) and the boundary limits defined in *params.py*. Once the mesh is obtained, the nodal connections possibilities are increased to enable smooth destinations composed from a sequence of edges. SIMROUTE nodes are connected by 48 edges, allowing 48 distinct directions per node (see Fig. 3) and enabling a smoothing of the sailing routes alternatives (Cheung, 2018) This enables angular courses of a range of $3.2^\circ - 14.0^\circ$ resolution to be obtained. Singular points on the mesh boundaries and corners are treated particularly to avoid non-defined mesh points when node searching. The initial and final nodes are defined also in *params.py* (see input variables in Fig. 1). These nodes are referred to the mesh computed previously; so a script is provided (i.e. *find_ports.py*) to convert the coordinates of the initial and final points, including checking to determine if the node is sea or land. Also, additional information is provided by this script in a command prompt for an iterative process on searching the initial and final nodes on the sea. The discrimination between either sea or land is given by the wave fields interpolated. Fig. 4 shows the mesh generated which the routes (i.e. minimum and optimal) are computed and an example of the interpolated significant wave height.

Because the CMEMS meshes and SIMROUTE mesh differ, the wave parameters (wave direction, wave period and significant wave height) from the CMEMS product are linearly interpolated in the computational mesh (see Fig. 4). Time resolution data are provided from CMEMS products (i.e. hourly or 3-hourly). The wave direction requires a

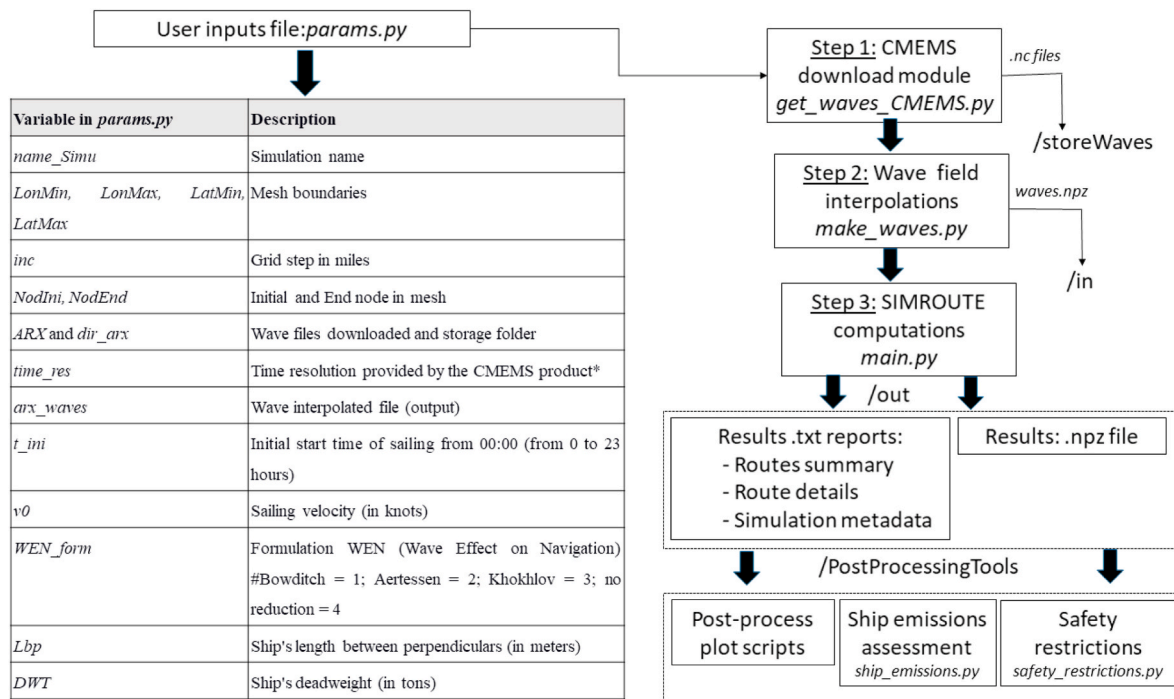


Fig. 1. Flow chart of SIMROUTE and list of input variables in *params.py*.

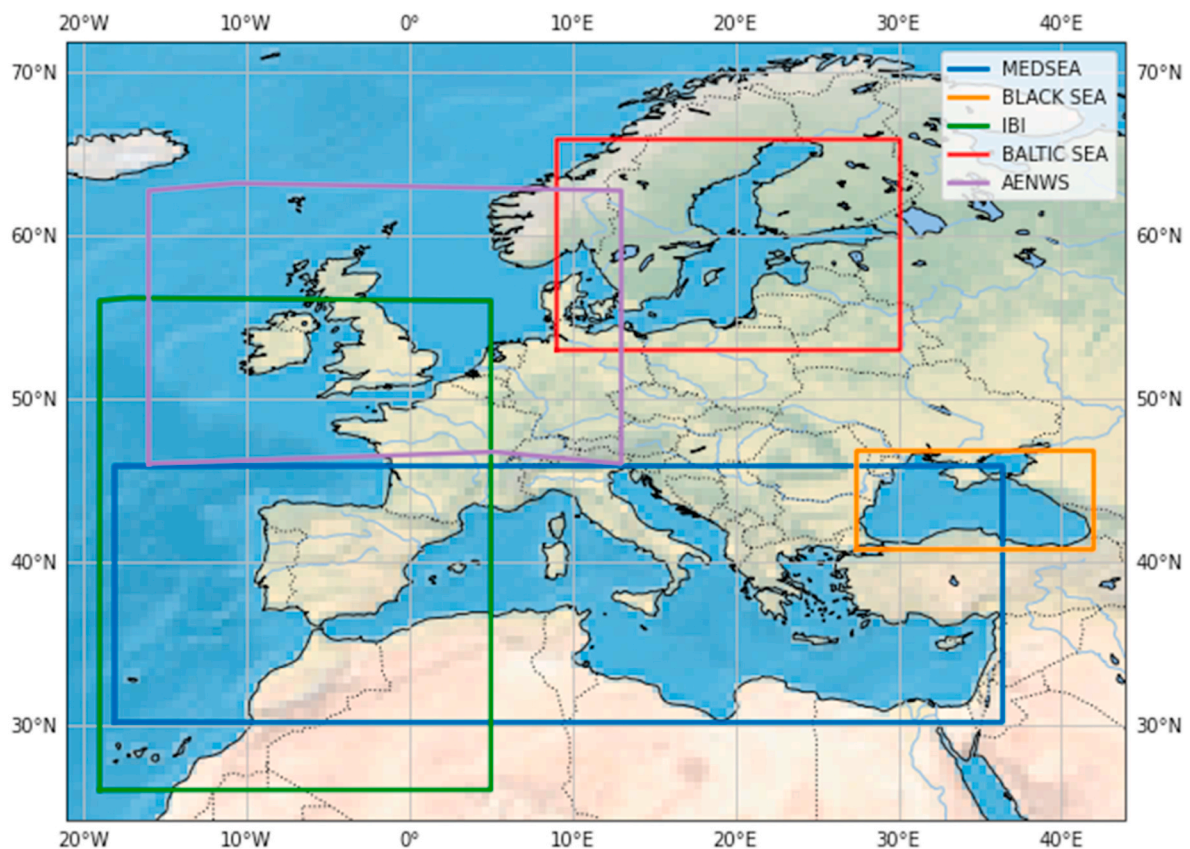


Fig. 2. CMEMS domains used in SIMROUTE. The legend shows the identification established in SIMROUTE software. The GLOBAL and ARCTIC domains are excluded in this figure.

Table 1

CMEMS products included in SIMROUTE system. * One-hour resolution for all domains except GLOBAL (3 h).

CMEMS Id.	Geographical covering	Spatial Resolution	wave_prod Flag	Reference
GLOBAL	Global Ocean	$0.083^\circ \times 0.083^\circ$	1	Ardhuin et al. (2010)
MEDSEA	Mediterranean Sea	$0.042^\circ \times 0.042^\circ$	2	Korres et al. (2021)
IBI	Iberia-Biscay-Irish Regional Seas	$0.05^\circ \times 0.05^\circ$	3	European Commission (2021)
AENWS	Atlantic European North West Shelf Seas	$0.03^\circ \times 0.014^\circ$	4	European Commission (2021)
BLACK SEA	Black Sea	$0.037^\circ \times 0.028^\circ$	5	(Staneva, J., Behrens, A., Ricker, M., & Gayer, 2020)
BALTIC SEA	Baltic Sea	2 km \times 2 km	6	European Commission (2021)
ARCTIC OCEAN	Arctic Ocean	3 km \times 3 km	7	European Commission (2021)

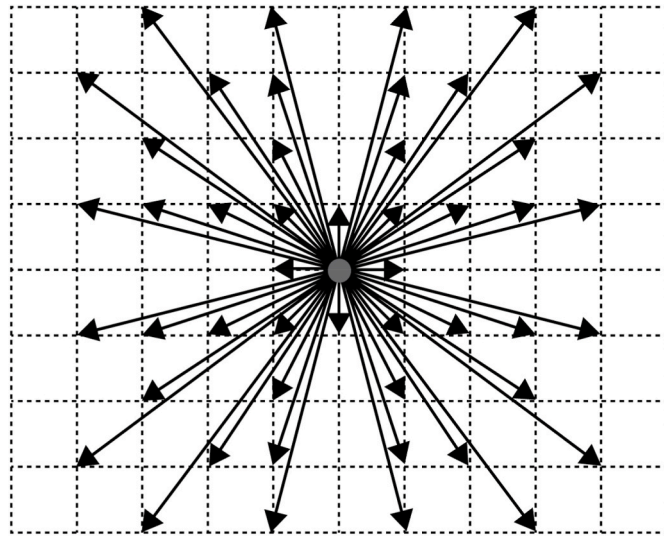


Fig. 3. Nodal connections and neighbouring scheme from departure mode (in grey).

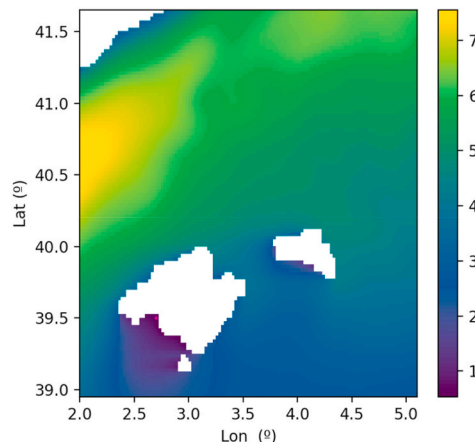
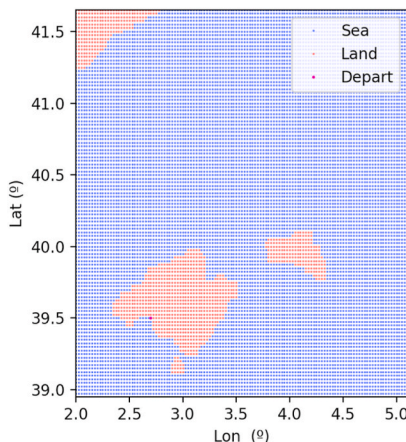


Fig. 4. Grid mesh generation and wave interpolation. The left-hand figure shows the mesh generated discerning between sea and land nodes (blue and orange respectively). The right-hand figure includes the significant wave height (H_s), in meters, interpolated on the mesh to ensure nodal location on a sea point. An eventual departure point is also shown in magenta. The region corresponds to Balearic Islands (NW Mediterranean Sea). (For interpretation of the references to colour in this figure legend, the reader is referred to the Web version of this article.)

particular interpolation based on Cartesian decomposition. The interpolated wave fields are saved on an intermediate file (*waves.npz* by default defined at *params.py*) in the *in/* folder. Route possibilities during ship routing computations are linked to the availability of wave information.

The wave, or sea state, parameters are essential in studies related to evaluations of the safety and fuel efficiency of marine designs and operations (Nielsen, 2021). In this contribution, the parametrization of the wave effect on navigation is based upon three methods, namely, Mannarini (suggested by Bowditch), Aertssen and Khokhlov (suggested by Lubkovsky) (Aertssen, 1975; Lubkovsky, 2009; Mannarini et al., 2013). All three methods depend on the significant wave height as well as the wave direction (see Appendix I). However, Aertssen's method also takes into account the ship's length dimension, whereas Khokhlov takes into account the deadweight of the ship (Borén et al., 2019) showed the discrepancies when using different calculation methodologies on ship routing in terms of the sailing time during storm episodes (large significant wave height). The Aertssen and Khokhlov methods give very similar results whereas the first method showed considerably higher values of ship velocity penalization due to waves. The ship-wave encounter direction is computed using an edge-based spherical method to preserve the coordinate system of the mesh.

2.3. Optimization algorithm

The pathfinding algorithm used is the A* algorithm due to its simplicity and efficiency in computational time. This algorithm is applied to a gridded scheme where each grid point (node) is connected to a set of adjacent points. To each connection (edge), a weight related to the distance is assigned. The great circle (orthodromic) track is used for the spherical coordinates of the grid nodes. A* solves problems by searching among all possible paths to the solution (goal) for the one that incurs the smallest cost (least distance travelled, shortest time, etc.), and among these paths, it first considers the ones that appear to lead most quickly to the solution. A* is formulated in terms of a weighted mesh: starting from a specific node of the mesh, it constructs a tree of paths starting from that node, expanding the paths one step at a time, until one of its paths ends at the predetermined goal node. At each iteration of its main loop, the A* algorithm needs to determine which of its partial paths to expand into one or more longer paths. It does this based on an estimate of the cost (in our case, the travel time) to reach the goal node. Specifically, A* selects the path that minimizes the total cost function $f(N_n)$:

$$f(N_n) = h(N_n) + \sum_{i=1}^n g(N_i) \quad (1)$$

where N_i denotes the i th nodes along the path candidate, $g(N_i)$ the cost of going from N_i to the parent $N_i - 1$, $h(N_n)$ is a heuristic that estimates the cost of the cheapest path from n to the goal (see Cheung, 2018 for a complete description). The heuristic allows longer paths to be eliminated progressively during the search. For the algorithm, to find the actual shortest path, the heuristic function must be admissible, meaning that it never overestimates the actual cost to get to the nearest goal node. The heuristic function used in SIMROUTE is the travelling time associated with the minimum distance between the origin and destination. When $h(N_n) = 0$, A^* reduces to the Dijkstra algorithm.

The accuracy of A^* implementation is tested by comparing with the orthodromic (or great-circle) distances. Different tests have been carried out in order to evaluate the error of the recovered path versus the analytical formula of the orthodromic distance in terms of the distance travelled. Four tests have been defined considering different positions (latitude and longitude) for the start and end point (see Table 2). Fig. 5 shows the shortest path estimated by A^* on the surface of a sphere for each of the test cases. The mesh grid is equal to 15 miles, substantially larger than the test cases shown in the next section. The distance travelled computed by A^* and the differences obtained compared with the orthodromic distance are shown in Table 2, in which differences less than 0.4% are obtained. The results guarantee a proper application of the shortest path algorithm used (i.e. A^*) embedded in SIMROUTE and its application for SWR problems.

2.4. Results files and post-processing

The SIMROUTE results information consists of two sets of files including the final and intermediate results and appropriate information to ensure an eventual simulation replication (see Fig. 1). On the one hand, a set of ASCII files (.txt) includes information of the cost function optimized (sailing time and distance including wave effect on navigation), minimum distance route, great circle distance and information to the start and end point, including departure time and mesh information (*Res_route.txt*). Metadata_route.txt includes information to replicate the simulation (e.g. wave fields, wave effect on navigation formulation, etc.). Finally, the file *Route_route.txt* includes the nodal information of the optimized route (longitude, latitude and wave conditions per each node visited by the optimized route). On the other hand, the .npz file (a file format by numpy Python library that provides storage of array data using gzip compression) is provided to allocate all the input/output variables of the simulation, including wave interpolated information. The simulation name, which is linked with the output file names, is provided also in *params.py* (see Fig. 1).

Post-processing tools are based on the .npz result file to ensure a decoupling of the simulation and post-processing analysis. Different graphical tools are oriented to provide comprehensive results including Lambert and Plate-Carrée projections. Also, the synchronous plotting or

Table 2

Numerical results of the orthodromic distance and shortest path distance (in nautical miles, nmi) comparison exercise shown in Fig. 5. The shortest path distance is estimated by A^* implemented in SIMROUTE code.

Case	Initial point (lon,lat)	Final Point (lon, lat)	Orthodromic Distance	Shortest path Distance	Difference in miles (Mean Absolute Percentage Error)
1	0°, 10N°	120°E, 10°N	7023.01	7038.25	15.24 (0.21%)
2	0°, 20N°	120°E, 20°N	6536.24	6549.36	13.12 (0.20%)
3	0°, 30N°	120°E, 30°N	5830.85	5845.51	14.66 (0.25%)
4	0°, 40N°	120°E, 40°N	4987.29	5005.56	18.27 (0.37%)

waves fields and routes are available using the Cartopy python library. Examples of post-processing tools based on test cases are displayed in Figs. 6–8.

2.5. SIMROUTE for academic purposes

From the academic point of view, ship weather routing and marine environment protection are specific topics in all Maritime Academies and Universities and related to the Seafarers' Training, Certification and Watchkeeping (STCW) Code (International Maritime Organization, 2010), as a part of mandatory training. Castells-Sanabra et al., 2019 identified which STCW competences the learner will achieve using SIMROUTE software, providing skills of ship routing optimization, to assess the impact of the meteo-oceanographic variables on ship navigation and to highlight the relevance of ship routing in terms of the sailing time, safety, fuel consumption and harmful emissions for the environment. Then, two academic modules were developed: i) safety restrictions and dangerous motions, and ii) ship emissions assessment. The SIMROUTE software is available for the academic community, together with comprehensive documentation and test cases oriented to guide teachers.

2.5.1. Safety restrictions module

The susceptibility of a vessel to dangerous phenomena will depend on the stability parameters, ship speed, hull shape and ship size. This means that the vulnerability to dangerous responses, including capsizing, and their probability of occurrence in a singular sea state may differ for each vessel. During navigation, unstable motions (surf-riding and parametric rolling) may be encountered, which may lead to a cargo or equipment damage and the unsafety of the persons on board. Safety restrictions to avoid surf-riding and parametric rolling are implemented into SIMROUTE according to the guidelines of the International Maritime Organization (International Maritime Organization, 2007) in order to know and avoid all the dangerous nodes from the route (see formulation in Appendix II). *safety_restrictions.py* is a post-processing tool to identify both dangerous unstable motions in the optimized route (see example in Fig. 9).

2.5.2. Ship emission module

A ship emission assessment module is included in SIMROUTE as a post-processing file. As an example, the emissions calculation methodology implemented in the SIMROUTE software is STEAM2 (Jalkanen et al., 2012), which takes into account the influence of the ship speed, engine load, fuel sulphur, multi-engine setups, abatement method and waves (see Appendix III for a short description of the formulation implemented in the ship emission module of SIMROUTE). (Borén et al., 2018) compared different emission assessment methodologies in the framework of route optimization and concluded that the STEAM2 methodology was the least factor-dependent methodology, since it depends on the type of fuel, specific fuel oil consumption and engine load. The STEAM2 model is combined with the power increase (ΔP) needed to overcome the speed penalization caused by the effect of waves on navigation (Δv) using the formula suggested by (Molland et al., 2017) as a function of the $P_{transient}$:

$$\frac{\Delta P}{P_{transient}} = \frac{1}{\left(1 - \frac{\Delta v}{v}\right)^3} - 1 \quad (2)$$

The new power (P_{new}) needed to overcome the adverse wave conditions is computed using the power transient conditions in each trip interval provided by the route simulator module.

$$P_{new} = P_{NSR} + \Delta P \quad (3)$$

where the P_{NSR} is then estimated from the engine load and power installed following the characteristics of the ship engine. Then, the total fuel consumption (FC) is calculated taking into account the sailing time

Table 3

Travel times (in hours) and distances (in nautical miles) and additional information of the CMEMS product test cases included in the repository. Min.: minimum distance route, Opt.: optimized route. H_s is the significant wave height.

Test case	CMEMS product	Min. Dist. time	Opt. time	Min. distance	Opt. distance	Max(H_s) Opt/Min (in m)	Emissions Savings (Min vs Opt)	Period of analysis	File in SIMROUTE repository
R1	MEDSEA	33.29	27.33	386.30	390.63	5.26/5.34	28.69%	13th-14th/01/2021	<i>params_MEDSEA_2.py</i>
R2	AENWS	38.64	37.85	539.12	544.38	4.23/4.17	4.47%	18th-19th/02/2020	<i>param_AENWS.py</i>
R3	GLOBAL	66.48	62.25	984.93	986.47	2.54/5.28	13.25%	18th-20th/04/2020	<i>param_GLOBAL.py</i>
R4	IBI	26.10	24.13	249.07	287.42	5.68/7.04	15.05%	16th-17th/02/2020	<i>param_IBI.py</i>
R5	GLOBAL	61.40	60.12	912.16	917.77	8.70/10.13	5.02%	8th-10th/08/2019	<i>param_GLOBAL_2.py</i>
R6	MEDSEA	16.93	14.97	151.38	161.56	6.95/6.85	16.14%	20th-21st/01/2020	<i>params_MEDSEA.py</i>
R7	BALTIC	17.47	17.43	266.64	266.88	2.73/2.86	0.61%	5th-6th/02/2020	<i>param_BALTIC.py</i>
R8	GLOBAL	187.04	183.60	2687.2	2725.9	6.00/6.44	4.42%	18th-25th/01/2020	<i>param_GLOBAL_3.py</i>

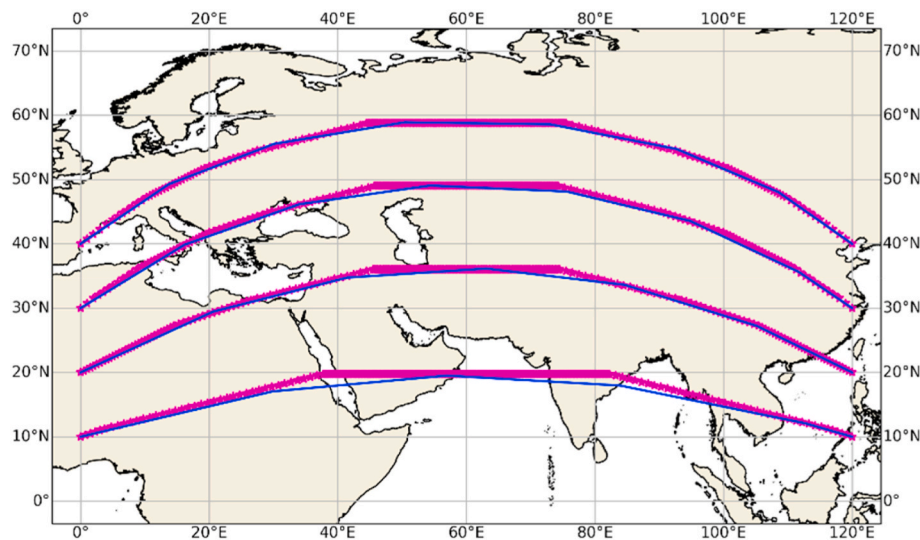


Fig. 5. Results for the Great Circle comparison exercise. Great-circle recovered by A* is plotted in magenta and great-circle estimated using Cartopy library from python is plotted in blue. The exact and estimated orthodromic distances are shown in Table 2. (For interpretation of the references to colour in this figure legend, the reader is referred to the Web version of this article.)

for the route. The script *ship_emissions.py* estimates the reduction in emissions of NOx, SOx, CO₂ and particulate matter (PM) between the minimum distance and the optimum route. The emissions are estimated at each node-to-node interval covering the optimum and the minimum distance route. The script generates an illustrative plot (see Fig. 10) together with an ASCII file with the ship emissions assessment.

Using SIMROUTE, Borén et al. (2022) investigated the emissions reduction for several scenarios covering the Western Mediterranean Short Sea Shipping routes (from 24 to 600 nautical miles and using a real Ro-Pax vessel). The ship routing optimization reveals a reduction up to 30% of ship emissions during severe storms on longer routes. Borén et al. (2022) also pointed out that the expected increase of extreme weather events, in terms of frequency, intensity and duration due to climate change, suggests a gradual gain of implementing ship weather routing optimization in all types of routes, regardless of the distance.

3. Results of the test cases

Different test cases are included in the SIMROUTE repository (with additional *params.py* files). These cases consider different regions using different CMEMS products. The study cases shown in Fig. 6 (Route 1),

Fig. 7 (Routes 2 to 7) and Fig. 8 (Route 8), including identification, are: (R1) the MEDSEA case which considers both shores of the Mediterranean Sea (Tunis/Nice); (R2) the European North-west Shelf (ENWS) product case (Hirtshals/Tórshavn); (R3) GLOBAL case focused on Japan coast (Hakodate/Kagoshima), (R4); IBI case (Santander/Lorient); (R5) the GLOBAL case applied to the North China Sea (Kaohsiung/Busan); (R6) the MEDSEA case (Palma de Mallorca/Barcelona); (R7) the BALTIC case (Gdynia/Stockholm) and (R8) the GLOBAL case applied to Atlantic routes (Boston/Plymouth). The R6 results and intermediate files are also included in the repository. The period analyzed, the distances sailed and the sailing time are summarized in Table 3, including the saving provided by the optimal route in comparison to the minimum distance route when only waves effect on navigation are considered. The emissions reduction percentage is also shown in this table. These cases pursue to present optimized routes using different CMEMS products and does not take into account relevant factors such as water depth, restricted area, piracy or territorial sea among others. User definition of these factors may be included as a non-sailing area manipulating the input netcdf files with specific tools such as Command Data Operators.

The maritime connection between Tunis and Nice (R1) shows the benchmark case in the MEDSEA domain, which considers both shores of

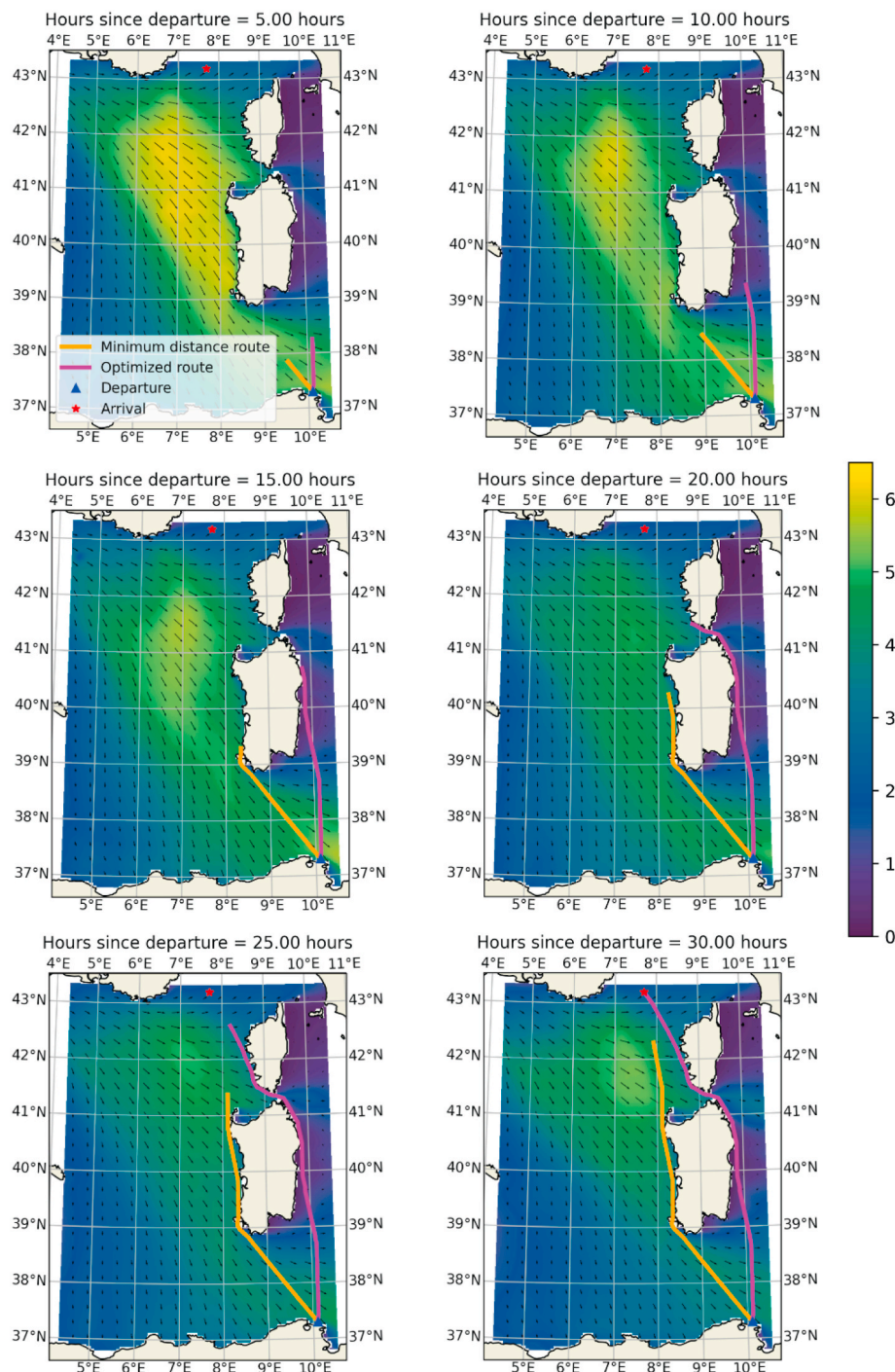


Fig. 6. Temporal sequence of the snapshot of the Tunis – Nice route (see parameters of the simulation in Table 3, R1). The optimal route is plotted in magenta and the minimum distance route is plotted in yellow. The colour bar represents the H_s (in meters) and the black arrows the direction of the waves synchronous with the ship routes evolution. (For interpretation of the references to colour in this figure legend, the reader is referred to the Web version of this article.)

the Mediterranean Sea with a ship speed of 16.1 knots. The temporal evolution of the optimal route (in magenta) and the minimum distance route (in yellow) from the MEDSEA case together with the sequence of the waves conditions are shown in Fig. 6. The simulation corresponds to the period of 13–14 January 2021. The optimal route recovered by SIMROUTE sailed via the eastern shore of Sardinia, avoiding the North-Westerly storm in the western Mediterranean Sea that was occurring in those days. In particular, the west Sardinia wave conditions suggested a head sea, which is the most penalizing condition of wave resistance in navigation, and also higher waves in comparison to the east shore. The

shorter sailing time is evidenced from the results in the optimized route in comparison to the minimum distance route (i.e. 27.33 h versus 33.29 h). This means that the route optimization shows that longer distance routes (i.e. 390.63 nmi vs 386.30 nmi) may be covered in less time. In this example the percentage of time saved is almost 18%. The AENWS-CMEMS product considers the route between Hirtshals (Denmark) and Tórshavn (Faroe Islands) (R2). Fig. 7a shows that the optimal route sails northward around the Shetland Islands in comparison to the minimum distance route. In this case, no substantial differences are obtained using SIMROUTE and the time-saving is equal to 2.1% (see Table 3). The

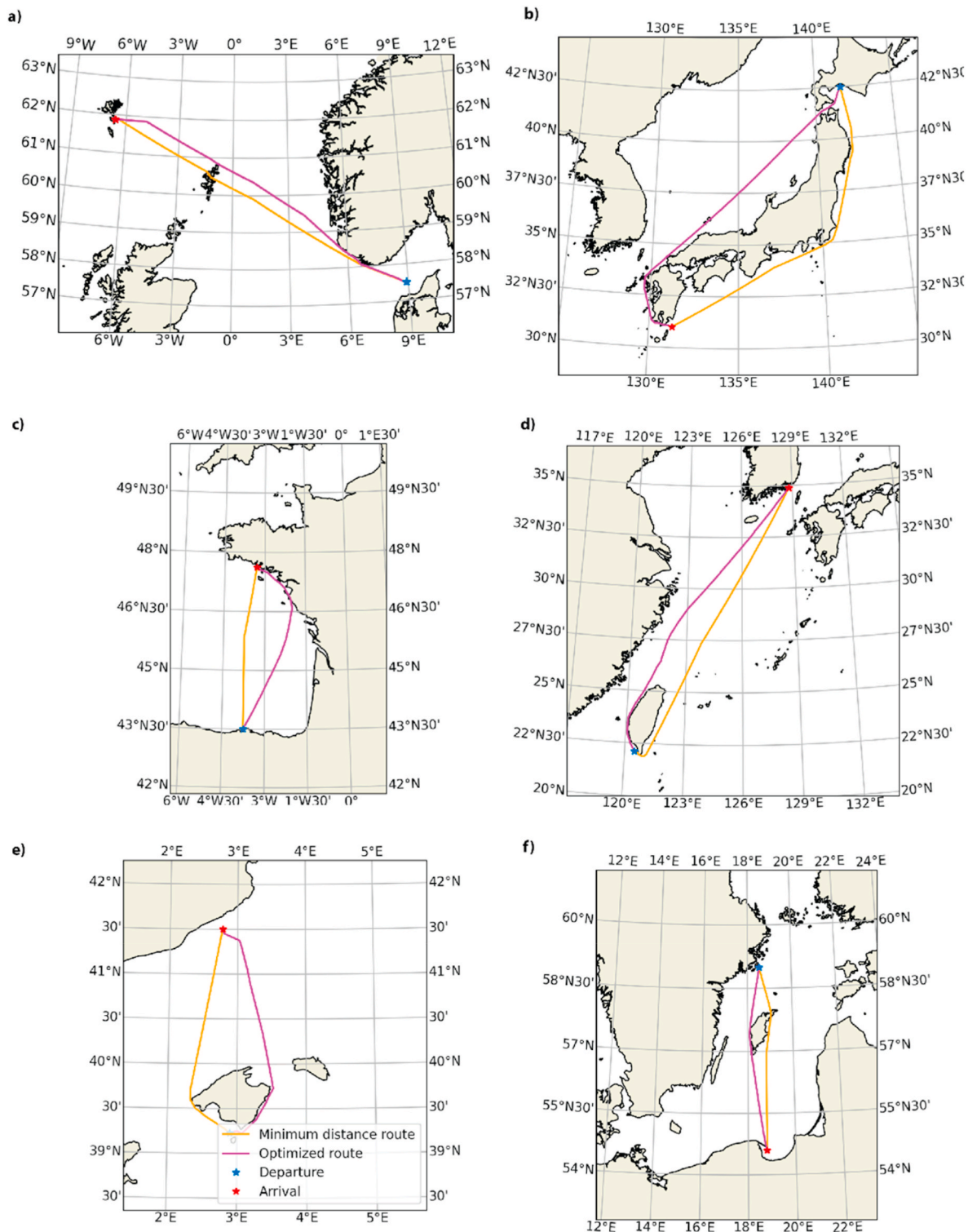


Fig. 7. Case test solutions (optimized and minimum distance routes) for different arrival/departure ports using different CMEMS products. a) R2: Hirtshals/Tórshavn, b) R3: Hakodate/Kagoshima, c) R4: Santander/Lorient, d) R5: Kaohsiung/Busan, e) R6: Palma de Mallorca/Barcelona and f) R7: Gdynia/Stockholm. (See detailed parameters and outputs of the simulation in Table 3, from R2 to R7).

GLOBAL-CMEMS product examples, covering the world seas, also suggest interesting results when SIMROUTE is applied. Fig. 7b shows an illustrative case for coastal shipping in Japan (i.e. Hakodate/Kagoshima, R3), for which the optimum route sails round the opposite coast of Honshu Island in comparison to the minimum distance route. In this case the time saving is equal to 6.36%. The IBI-CMEMS product example includes a route between Santander and Lorient (Fig. 7c, R4). In this case

the time saving is equal to 7.55% and the optimal route sails near the coast to avoid large significant wave height values of the Bay of Biscay. The shipping connection between Kaohsiung (Taiwan Island) and Busan (Korea) sailing the East China Sea (Fig. 7d, R5) also shows substantial differences between the minimum distance and optimal route (time-savings equal to 2.08%). Also, short shipping activities (less than 200 nmi) may reveal substantial differences, as in the case of the connection

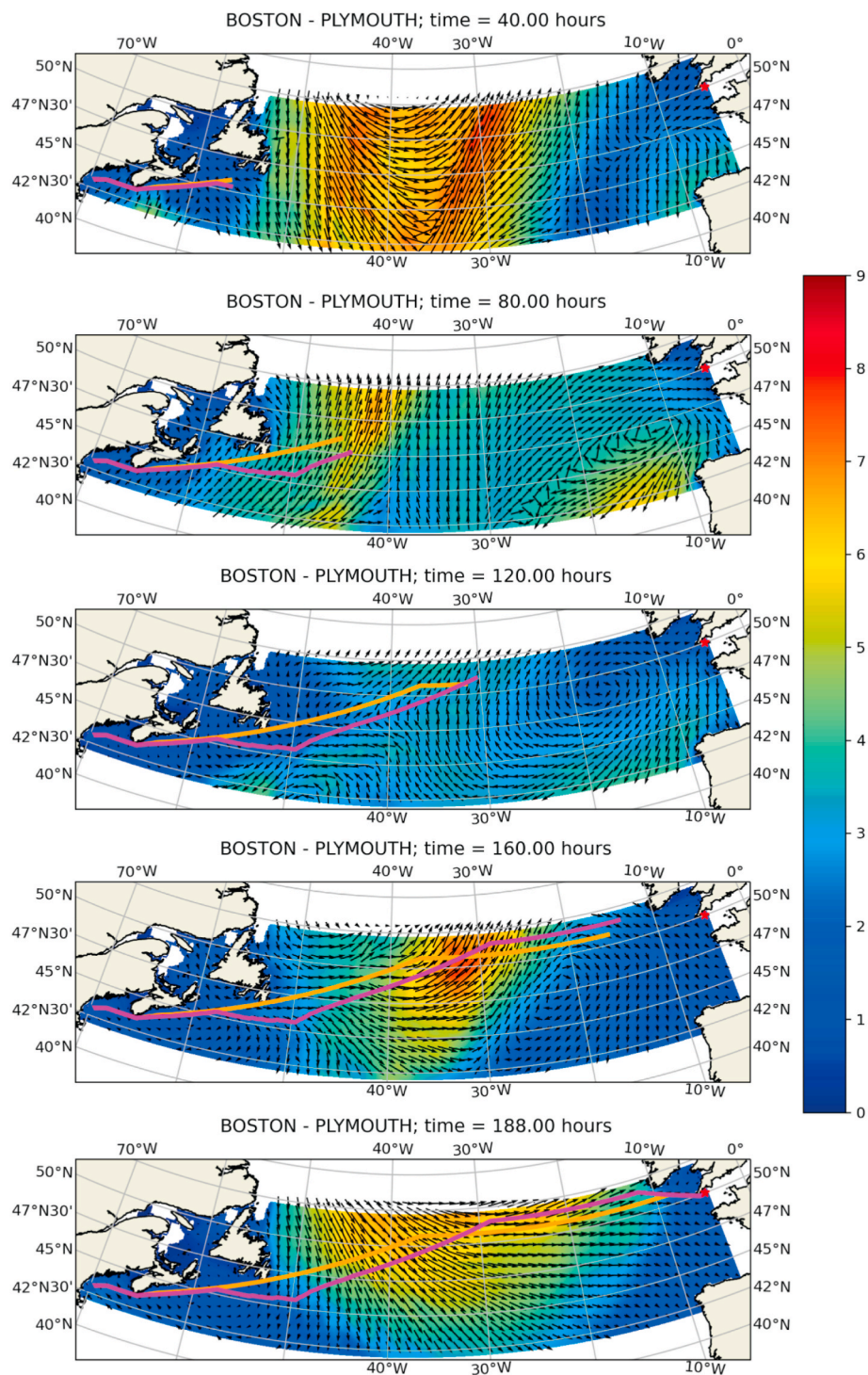


Fig. 8. Temporal sequence of the case of Boston – Plymouth (see parameters of the simulation in Table 3, R8). The optimal route is plotted in magenta and the minimum distance route in yellow. The colour bar represents the H_s (in m) and the black arrows the direction of the waves synchronous with the route simulation. (For interpretation of the references to colour in this figure legend, the reader is referred to the Web version of this article.)

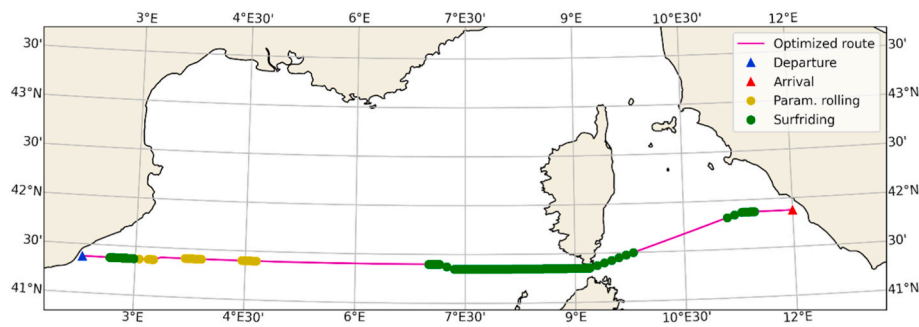


Fig. 9. Example of *safety_restrictions.py*: surf-riding and parametric rolling over the optimized route.

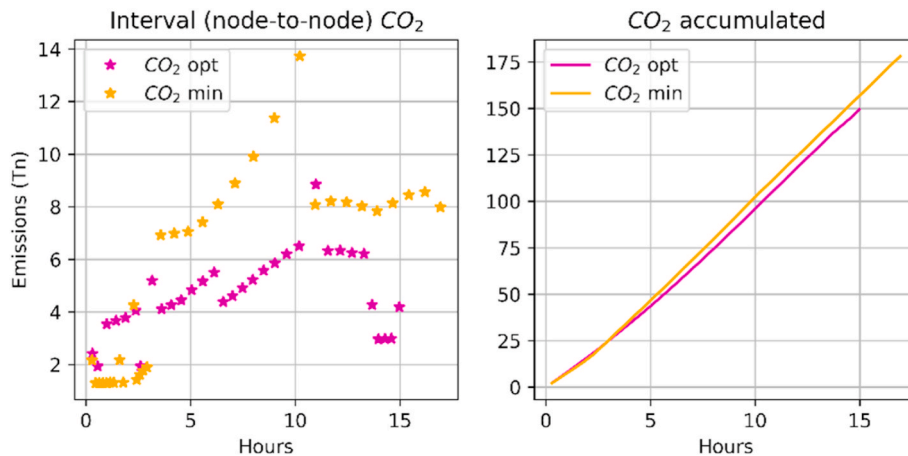


Fig. 10. Interval (node-to-node) and accumulated CO₂ emissions (in Tn) for minimum (orange) and optimum (magenta) route for the case of Palma de Mallorca – Barcelona. The optimal and minimum distance routes are shown in Fig. 7e. (For interpretation of the references to colour in this figure legend, the reader is referred to the Web version of this article.)

between Mallorca Island and Barcelona for MEDSEA-CMEMS (R6). In general, the cases shown previously correspond to large significant wave height values entailing substantial differences between the minimum and optimal routes.

Table 3 also includes information about the maximum significant wave height faced by both routes. In general, the maximum significant wave height is reduced for the optimum route in agreement with the results shown in Fig. 6. However, in the fetch restricted seas, such as the Baltic Sea, large significant wave height values may induce the optimal route to be detached from the minimum distance route. In the BALTI-CMEMS product case between Gdynia and Stockholm (R7, Fig. 7f), the maximum H_s during the optimum trip is equal to 2.73 m; for these wave conditions the optimal route recovered by SIMROUTE suggests a western sailing route of Gotland Island in comparison to the minimum distance route. During calm periods, the differences are not relevant and the minimum optimal route is the same as the minimum distance route. Note that the wave information shown in Table 3 reveals substantial wave conditions for both the minimum distance and optimized routes in many cases (e.g. Santander/Lorient (R4) or Hakodate/Kagoshima (R3)). Based on the time cost reduction provided by SIMROUTE, ship emission reductions are also assessed according to section 2.5.2. Emissions reductions range from 0.61% to 28.69%, consistent with the time-saving (see Table 3).

Finally, Atlantic routes that connect Europe and the USA East coast also provide interesting insights. These routes have been investigated in previous publications (e.g. (Hinnenthal and Clauss, 2010; Shao et al., 2012)), revealing noticeable differences due to the typical adverse weather conditions in the North Atlantic. Fig. 8 shows the route between Boston (USA) and Plymouth (UK) obtained by SIMROUTE, where substantial differences are revealed (183.6 h for the optimized route vs.

187.0 h for the minimum distance route, which is a reduction of 9.1%) using GLOBAL-CMEMS products. In this sense SIMROUTE provides a smart route avoiding bad weather conditions (an illustrative snapshot is shown for the hour 80, when the optimal route sails southward in comparison to the minimum distance route).

4. Discussion

SIMROUTE code execution includes a few sequential steps and a unique input file enabling comprehensive use by the practitioner and easy learning in ship route optimization methods. Recently (Zis et al., 2020b), highlighted the increasing attention in similar problems on finding the optimal path and sailing speed considering environmental conditions. In addition, they suggested a standardization of methods to facilitate inter-comparison of methodologies. In this respect, SIMROUTE fills the gap, providing an open, comprehensive and efficient software to compute weather ship routes using CMEMS products, and it seems a good candidate for a benchmarking strategy. For instance, the inclusion of input variables in a unique file enables easy implementation for new cases and the modification of input variables testing different scenarios.

Wave interpolation is still highly time-consuming, so the use of the A* algorithm and the possibility to run the code in unix platforms makes the use of SIMROUTE feasible for long distances (e.g. see the GLOBAL-CMEMS cases shown in the previous section). Taking into account the different methods presented in the Introduction section, multi-objective methods suggest robust optimized solutions for a few objectives, such as the minimum time of arrival, navigation risk and minimum fuel consumption etc. (e.g. Hinnenthal and Clauss, 2010; Zhao et al., 2022); although the solution is highly dependent on the population size of the initial generation of solutions requiring large computing resources

(Simonsen et al., 2015). Accurate objectives parametrization is required in multi-objective weather routing systems (Zhao et al., 2022), which may add complexity and uncertainty on new implementations. Also, other methods faced the route optimization in terms of fuel consumption (e.g. (Takashima and Mezaoui, 2009)). In those terms, it should be highlighted that the present contribution takes into account the non-linearity in the relation between fuel consumption and engine load. This relation is considered to have an approximately parabolic dependency and the change on Specific Fuel Oil Consumption (SFOC) is assessed over whole route. Therefore, SFOC is calculated for the different conditions which the vessel is facing in each node and total fuel consumption is obtained through the relation among instantaneous power, SFOC and the interval time from node to node. As future works, for the sake of fuel consumption estimation accuracy, other determinants could be taken into account such as vessel's draught, trim or water depth inter alia.

However, all methods present benefits and deficiencies as a function of the problem statement (single or multiple), computational resources and simulation performance. SIMROUTE pursues a trade-off between accuracy, user-friendliness and computational time, assuming standard computational resources. In this respect, the current version of the code uses simple added wave resistance models instead of formulations based on specific transfer functions, spectrum-based resistance or reduced non-dimensional resistance for calm and added wave resistance (Hinnenthal and Clauss, 2010; Hu et al., 2014; Mannarini et al., 2016). This allows an easy interpretation of the wave effect on navigation using velocity penalization formulations (see inter-comparison exercise in (Borén et al., 2019)). Also, the modular structure of SIMROUTE suggests an easy implementation of more complex wave resistance formulations and other resistance factors such as the effects of wind, water currents or sea-ice on navigation (see formulations in (Cai and Wen, 2014)). For instance, the use of additional CMEMS products (and also ERA5 for wind description), may be a good start point to include these factors on ship resistance to navigation. These topics, some of them included in beta versions of SIMROUTE, are considered as future works. Also, the effect of the added resistance formulations may have a direct effect on the fuel consumptions and ship emissions, so future works also include sensitivity analysis of all these factors including the emissions formulations itself (STEAM2) which under specific circumstances may differ from real values (Berthelsen and Nielsen, 2021).

The IMO resolution A.528(13) (International Maritime Organization, 1983) recommends to Governments to advise ships to make use of weather routing information. In this sense, several commercial products have been developed in the field of maritime routing but with limited available information on the underlying methodologies. As pointed out by Zis et al. (2020a), these systems are operating as black boxes with suggestions on the optimal route with lack of transparency on optimizations and information processed. In opposite, the open-software philosophy on SIMROUTE could trigger a wide cooperation for the development of weather routing systems, both at the industrial and the academic level, in compliance with the most recent e-navigation instances.

The software provided and additional analysis may fit in an operational oceanography context (e.g. emissions or safety on navigation) as a contribution to efficient and safe maritime operations such as route plan design based on wave forecast products. SIMROUTE is based on waves CMEMS products, which provides free and open marine data including learning services, enabling maritime routes in different domains including global areas. In this sense, SIMROUTE provides for the first time a model which include the world application area and sub-regional domains (see review paper in Simonsen et al., 2015 and Zis et al., 2020a). Also the portability of netcdf files for wave information makes it very easy to include new wave products in SIMROUTE from other regional and downstream services (e.g. Sotillo et al., 2020). The accuracy and impact of SWR will also benefit from the future improvement of weather forecasting in terms of accuracy and spatio-temporal

description. In this respect, the extension of the forecast horizon will permit long-haul routes and multi-port vessel routes to be addressed.

As a function of the wave conditions, SIMROUTE may provide a limited extension to the benefits of the optimized route and the minimum distance route. The results shown in the previous section have revealed that calm sea conditions or moderate storms may have an imperceptible impact on the optimized route in comparison to the minimum distance. However, the real routes may be far from the minimum distance routes, increasing the relevance of the SWR results. New implementations using SIMROUTE should be designed previously taking into account the forecast horizon of the wave products, the sailing duration and the consequences of grid spacing resolutions that may increase substantially the computational cost. As future work, AIS routing inter-comparison will suggest an increase of the importance of SWR, with a direct impact on emissions reduction or economic benefits, using frequent commercial shipping routes. Complementary analysis with SIMROUTE allows the exploration of optimized routes in a wide framework, such as ship emissions evaluation or new routes such as the North Sea passage. Finally, the emergence of autonomous vessels requires specific new route design systems, including safety, fuel efficiency, emissions and efficient routes (Wu et al., 2021; Zakaria et al., 2022; Zis et al., 2020b). As noted by (Zis et al., 2020b), research on SWR in world navigation will be a topic deserving ever more attention in the coming years as the world pursues greenhouse emissions reduction, the blue economy and sustainable development. In this sense, SIMROUTE provides a robust alternative for SWR analysis and development in an open and collaborative perspective.

5. Conclusions

We describe a comprehensive and free software for Ship Weather Routing referred to as SIMROUTE. The code targets one of the aspirations of ship weather routing by minimizing time of navigation and, in consequence fuel consumption and emissions. SIMROUTE uses the A* pathfinding algorithm and pursues a trade-off between accuracy, user-friendliness and computational time, assuming standard computational resources. Several cases using different CMEMS products over short and long distances including ship emission assessment have been tested. SIMROUTE provides a robust alternative for Ship Weather Routing analysis and development in an open and collaborative perspective.

Funding

This work was partially supported by MObiLity sERvices Enhanced by GALILEO & Blockchain, MOLIERE (H2020 5th call, Contract Number: 101004275).

Author contributions

Conceptualization, M.G.; methodology, M.G. and C.B.; software development: M.G. and C.B.; investigation, C.B. and M.C.; writing-original draft preparation, M.G.; writing-review and editing, M.C. and C.B.; visualization, M.G. and M.C.; Supervision; M.G. and M.C. All authors have read and agreed to the published version of the manuscript.

Declaration of competing interest

The authors declare that they have no known competing financial interests or personal relationships that could have appeared to influence the work reported in this paper.

Acknowledgements

The authors acknowledge CMEMS (Copernicus Marine Environment Monitoring Service) for the wave predictions provided.

Appendix I. Wave effect on navigation formulation

SIMROUTE considers three formulations for the assessment of the wave effect on navigation. The first method implemented into the weather routing system to analyze the vessel speed reduction due to wave effect according to [Mannarini et al., 2013](#)) (inspired by Bowditch (2002)). The final speed is computed in function of the non-wave affected speed (v_0) plus a reduction in function of the wave parameters:

$$v(H_s, \theta) = v_0 - f(\theta) \cdot H_s^2 \quad (\text{A1.1})$$

where v_0 is the vessel initial speed without wave effect, H_s is the significant wave height and θ is the ship-to-wave relative direction (clockwise).

Table A1.1
Values of f coefficient

θ	$f(\text{in kn/ft}^2)$
$0^\circ \leq \theta \leq 45^\circ$	0.0083
$45^\circ < \theta < 135^\circ$	0.0165
$135^\circ \leq \theta \leq 225^\circ$	0.0248
$225^\circ < \theta < 270^\circ$	0.0165
$270^\circ \leq \theta \leq 360^\circ$	0.0083

The second methodology implemented into the SWR is Aertssen's formula ([Aertssen, 1975](#)). Aertssen's formula also takes into account the ship's dimensions, in particular, the ship's length. For approximating the speed reduction, Aertssen proposes the following equation:

$$v = v_0 - \left(\frac{m}{L_{BP}} + n \right) \frac{v_0}{100} \quad (\text{A1.2})$$

where L_{BP} is vessel's length between perpendiculars and m and n are empirical coefficients defined in [Table A1.2](#).

Table A1.2

Values of m and n Aertssen coefficients depending on the wave characteristics (BN= Beaufort number, H_s = significant wave height, W_{speed} = wind speed)

BN	H_s	θ W_{speed}	150°-210°		60°-150° / 210°- 300°		30°-60° / 300°- 330°		0°-30° / 330°- 360°	
			m	n	m	n	m	n	m	n
5	2.5	17–21	900	2	700	2	350	1	100	0
6	4.0	22–27	1300	6	1000	5	500	3	200	1
7	5.5	28–33	2100	11	1400	8	700	5	400	2
8	7.5	34–40	3600	18	2300	12	1000	7	700	3

The columns of the table contain estimated values of m and n coefficients for waves hitting a vessel at a particular angle θ in degrees.

Khokhlov formula is suggested by [Lubkovsky \(2009\)](#). This method takes into account the height and direction of the waves and also the ship's dimensions, in particular, the deadweight of the ship. According to ([Maisiuk and Gribkovskaia, 2014](#)) the standard error for this formula does not exceed 0.5 knots. Khokhlov method calculates speed reduction as follows:

$$v = v_0 - (0.745 \cdot H_s - 0.245 \cdot \theta \cdot H_s) \cdot (1.0 - 1.35 \cdot 10^{-6} \cdot D \cdot v_0) \quad (\text{A1.3})$$

where θ (here in radians) and D is vessel's deadweight (DWT) in tons. Khokhlov method is applicable for vessels with a deadweight range from 4.000 to 20.000 DWT including supply vessels, and design speeds between 9 and 20 knots.

Appendix II. Safety restrictions formulation

The methodology used in SIMROUTE to assess safety restrictions takes into account the recommendations of the International Maritime Organization ([International Maritime Organization, 2007](#), circular no. 1228) for avoiding dangerous situations in adverse weather and sea conditions ([Krata and Szlapczynska, 2018](#); [Mannarini et al., 2013](#)). Two unstable motions that can cause discomfort to the passage and crew members, generating dynamic loads to the structure and cargo of the ship are implemented into SIMROUTE: surf-riding and parametric rolling.

When a ship is situated on the steep forefront of a high wave in following or quartering sea conditions, the ship can be accelerated to ride on the wave. This is known as surf-riding. In this situation the so-called broaching-to phenomenon may occur, which endangers the ship to capsizing as a result of a sudden change of the ship's heading and unexpected large heeling. Surf-riding and broaching-to may occur when both of these conditions are fulfilled:

$$135^\circ < \alpha < 225^\circ \quad (\text{A2.1})$$

and

$$v > \frac{1.8 \sqrt{L_{\text{ship}}}}{\cos(180^\circ - \alpha)} \quad (\text{A2.2})$$

where α is the angle of encounter, being the ship-to-wave relative direction ($\alpha = 180^\circ$ for following seas), L_{ship} is the length of the ship in meters and v is the speed of the ship in knots.

On the other hand, parametric roll motions with large and dangerous roll amplitudes in waves are due to the variation of stability between the position on the wave crest and the position in the wave trough. Parametric rolling may occur in two different situations:

$$|T_E - T_R| = \varepsilon \cdot T_R \quad (A2.3)$$

or

$$|2 \cdot T_E - T_R| = \varepsilon \cdot T_R \quad (A2.4)$$

where ε is the relative tolerance in frequency matching in %, T_E is the encountered period with waves in seconds and T_R is the natural roll period in seconds. The method for calculation of the natural roll period is given in the Intact Stability Code and is based on the initial metacentric height of a ship (International Maritime Organization, 2008).

Appendix III. Ship emission formulation

The methodology used in SIMROUTE (i.e. STEAM2) to estimate emissions was inspired by a Theoretical Based Method (TBM) with a bottom-up approach, that obtains their results via modelling with no data recorded on-board (Borén et al., 2018). This TBM, which includes input variables such as installed power per engine or engine load, was successfully applied in Ro-Pax ships by (Jalkanen et al., 2009) and (Jalkanen et al., 2012). STEAM2 methodology allows the evaluation of the exhaust emissions of marine traffic based on the messages provided by the Automatic Identification System (AIS). The evaluation of (Jalkanen et al., 2009) and (Jalkanen et al., 2016) in SWR was already discussed in (Borén et al., 2018) concluding that this method uses ship specific data to obtain more accurate calculations as it is a bottom-up methodology. The required data for emissions assessment and main assumptions for the ship emission assessment are shown in Table A3.1.

Table A3.1

Required data for emission assessment methodology in SIMROUTE.

Input data	Acronym	Assumptions
Installed power per engine (in kW)	$P_{Installed}$	From IHS Markit database
Engine Load	EL	According to (Jalkanen et al., 2012), EL's values are around 70%–80%
Specific Fuel Oil Consumption (in g/kWh)	$SFOC$	From the corresponding manufacturer's project guide of the engine
Design speed (in knots)	V_{design}	From IHS Markit database
Sulphur and Carbon Content of fuel (in mass percentage)	SC/CC	Depends on the fuel burnt
Main Engine Revolutions per Minute (in rpm)	rpm	If engine data is unavailable, the ship is assumed to use a 500 rpm medium speed diesel engine by default
Molar mass of Sulphur/Sulphur dioxide/Carbon/Carbon dioxide (in g/mol)	$M(S)/M(SO_2)/M(C)/M(CO_2)$	

Total emissions for each pollutant (E_{Tp}) per ship and per route is the sum of the amount of pollutant (p) emitted into the atmosphere and can be obtained by applying the following formula, changing the emissions factor related to one pollutant or another:

$$E_{Tp} = P \cdot EL \cdot EF_p \cdot t \quad (A3.1)$$

where P is the average output power (in kW), EL is the engine load, EF is the emission factor of each pollutant (according to Table A3.1) and t (in hours) is the total time sailed.

Table A3.2

Summary table of the EF for each pollutant.

Sulphur dioxide (SO_2)	$EF(SO_2) = M(SO_2)nn(SO_2) = M(SO_2)nn(S) = M(SO_2)n \frac{SFOCnSC}{M(S)} \text{ (g/kWh)}$
Carbon dioxide (CO_2)	$EF(CO_2) = M(CO_2)nn(CO_2) = M(CO_2)nn(C) = M(CO_2)n \frac{SFOCnCC}{M(C)} \text{ (g/kWh)}$
Nitrogen oxides (NO_x)	$\begin{cases} 17(rpm < 130) \\ 45^{rpm-0.2} (130 < rpm < 2000) \\ 9.8(rpm > 2000) \end{cases}$
Particulate Matter (PM)	$EF(PM) = SFOC_{REL}(EF_{SO_4} + EF_{H_2O} + EF_{OC}OC_{EL} + EF_{EC} + EF_{ASH})$ Where: $SFOC_{REL} = 0.455EL^2 - 0.71EL + 1.28$; $SFOC = SFOC_{REL}nSFOC_{MANUFACTURER}$

The total amount of each pollutant emission can be assessed by adapting equation (A3.1) to the pollutant analyzed, as shown below:

$$E_{Tp} = \sum_{i=0}^n P_i^{new} \cdot EL_i^{new} \cdot EF_{(p)i} \cdot \Delta t_i \quad (A3.2)$$

Obtaining P^{new} and n being the number of intervals i and Δt the time from node-to-node for each interval.

In order to estimate the impact of Engine Load (EL) change on Specific Fuel Oil Consumption ($SFOC$), the EL for each interval was calculated (EL^{new}):

$$EL^{new} = P^{new} / P_{Installed} \quad (A3.3)$$

These formulas assumed that there is a linear relation between fuel consumption and EL , and $SFOC$ is presumed to be constant. Through manufacturers data, it can be seen that $SFOC$ is a non-linear function of EL but that there is an approximately parabolic dependency between them. STEAM2 assumes a parabolic function for all engines getting to following equations for relative $SFOC$ ($SFOC_{rel}^{new}$) and final $SFOC$ ($SFOC_{end}$) using regression analysis:

$$SFOC_{rel}^{new} = 0.445 \cdot (EL^{new})^2 - 0.71 \cdot EL^{new} + 1.28 \quad (A3.4)$$

$$SFOC_{end} = SFOC_{rel}^{new} \cdot SFOC \quad (A3.5)$$

Afterwards, the absolute fuel consumption (FC) was estimated as follows:

$$FC = \sum_{i=0}^n P_i^{new} \cdot SFOC_i^{new} \cdot \Delta t_i \quad (A3.6)$$

References

- Aertssen, G., 1975. The effect of weather on two classes of container ships in the North Atlantic. *Nav. Archit.* 11–13.
- Ardhuin, F., Magne, R., Filipot, J.-F., Van, A., Westhuysen, D., Roland, A., Queffelecoul, P., Lefevre, J.-M., Aouf, L., Babanin, A., Collard, F., 2010. Semi-empirical dissipation source functions for wind-wave models: part I, definition, calibration and validation at global scales. *J. Phys. Oceanogr.* 40.
- Berthelsen, F.H., Nielsen, U.D., 2021. Prediction of ships' speed-power relationship at speed intervals below the design speed. *Transport. Res. Transport Environ.* 99, 102996 <https://doi.org/10.1016/j.trd.2021.102996>.
- Borén, C., Castells-Sanabra, M., Grifoll, M., 2022. Ship emissions reduction using weather ship routing optimisation. *J. Eng. Maritime Environ.* 1–12. <https://doi.org/10.1177/14750902221082901>.
- Borén, C., Castells-Sanabra, M., Grifoll, M., 2018. Intercomparison of emissions assessment methodologies in a short sea shipping framework. In: 19th International Association of Maritime Universities Annual General Assembly, International Center for Numerical Methods in Engineering (CIMNE), pp. 416–424.
- Borén, C., Falevitch, L., Castells-Sanabra, M., Grifoll, M., 2019. Added resistance parametrizations due to waves in a weather ship routing system. In: International Conference of Maritime Science & Technology NASE MORE, International Conference of Maritime Science & Technology NASE MORE 2019, pp. 50–59.
- Cai, Y., Wen, Y., 2014. Ship route design for avoiding heavy weather and sea conditions. *TransNav, Int. J. Mar. Navig. Saf. Sea Transp.* 8, 551–556. <https://doi.org/10.12716/1001.08.04.09>.
- Castells-Sanabra, M., Borén, C., Grifoll, M., Martínez de Osés, F.X., 2019. Weather Routing Software for academic purposes A pilot study. In: Proceedings of Teh International Association of Maritime Universities (IAMU).
- Chapman, L., 2007. Transport and climate change: a review. *J. Transport Geogr.* 15, 354–367. <https://doi.org/10.1016/j.jtrangeo.2006.11.008>.
- Cheung, J.C.H., 2018. Flight planning: node-based trajectory prediction and turbulence avoidance. *Meteorol. Appl.* 25, 78–85. <https://doi.org/10.1002/met.1671>.
- DfT, 2004. The Future of Transport: A Network for 2030, Cm (Series) (Great Britain. Parliament). Stationery Office.
- European Commission, 2021. Copernicus Marine Environmental Monitoring Service [WWW Document]. URL: <https://www.copernicus.eu> (accessed 4.1.20).
- Goldsworthy, L., Goldsworthy, B., 2015. Modelling of ship engine exhaust emissions in ports and extensive coastal waters based on terrestrial AIS data - an Australian case study. *Environ. Model. Software* 63, 45–60. <https://doi.org/10.1016/j.envsoft.2014.09.009>.
- Grifoll, M., Martínez de Osés, F.X., 2016. A ship routing system Applied at Short Sea distances. *XIII J. Marit. Res.* 3–6.
- Grifoll, M., Martínez de Osés, F.X., Castells, M., 2018. Potential economic benefits of using a weather ship routing system at Short Sea Shipping. *WMU J. Marit. Aff.* 17, 195–211. <https://doi.org/10.1007/s13437-018-0143-6>.
- Hagiwara, H., 1982. Weather Routing of (Sail-assisted) Motor Vessel.
- Hinnenthal, J., Clauss, G., 2010. Robust Pareto-optimum routing of ships utilising deterministic and ensemble weather forecasts. *Ships Offshore Struct.* 5, 105–114. <https://doi.org/10.1080/17445300903210988>.
- Hu, Q., Cai, F., Yang, C., Shi, C., 2014. An algorithm for interpolating ship motion vectors. *TransNav, Int. J. Mar. Navig. Saf. Sea Transp.* 8, 35–40. <https://doi.org/10.12716/1001.08.01.04>.
- International Maritime Organization, 2010. International Convention on Standards of Training, Certification and Watchkeeping for Seafarers (STCW). London, UK.
- International Maritime Organization, 2008. International code on Intact stability. Resolut. MSC 267 (85).
- International Maritime Organization, 2007. Annex A IMO Circular MSC.1/Circ. 1228 Dated 11 January 2007.
- International Maritime Organization, 1983. Resolution A.528(13) Adopted on 17 November 1983 Recommendation on Weather Routeing 528.
- Jalkanen, J.-P., Johansson, L., Kukkonen, J., 2016. A comprehensive inventory of ship traffic exhaust emissions in the European sea areas in 2011. *Atmos. Chem. Phys.* 16, 71–84. <https://doi.org/10.5194/acp-16-71-2016>.
- Jalkanen, J.P., Brink, A., Kalli, J., Pettersson, H., Kukkonen, J., Stipa, T., 2009. A modelling system for the exhaust emissions of marine traffic and its application in the Baltic Sea area. *Atmos. Chem. Phys.* 9, 9209–9223. <https://doi.org/10.5194/acp-9-9209-2009>.
- Jalkanen, J.P., Johansson, L., Kukkonen, J., Brink, A., Kalli, J., Stipa, T., 2012. Extension of an assessment model of ship traffic exhaust emissions for particulate matter and carbon monoxide. *Atmos. Chem. Phys.* 12, 2641–2659. <https://doi.org/10.5194/acp-12-2641-2012>.
- Kanellos, F., Prousalidis, J.M., Tsekouras, G.J., 2014. Control system for fuel consumption minimization–gas emission limitation of full electric propulsion ship power systems. *Proc. Inst. Mech. Eng. Part M J. Eng. Marit. Environ.* 228, 17–28. <https://doi.org/10.1177/1475090212466523>.
- Korres, G., Ravdas, M., Zacharioudaki, A., Denaxa, D., Sotiropoulou, M., 2021. Mediterranean Sea Waves Analysis and Forecast (CMEMS MED-Waves, MedWAM3 System) (Version 1) [Data Set]. Copernicus Monitoring Environment Marine Service (CMEMS). https://doi.org/10.25423/CMCC/MEDSEA_ANALYSISFORECAST_WAV_006_017_MEDWAM3.
- Krata, P., Szlapczynska, J., 2018. Ship weather routing optimization with dynamic constraints based on reliable synchronous roll prediction. *Ocean Eng.* 150, 124–137. <https://doi.org/10.1016/j.oceaneng.2017.12.049>.
- Kuhlemann, S., Tierney, K., 2020. A genetic algorithm for finding realistic sea routes considering the weather. *J. Heuristics* 26, 801–825. <https://doi.org/10.1007/s10732-020-09449-7>.
- Lin, Y.-H., Fang, M.-C., Yeung, R.W., 2013. The optimization of ship weather-routing algorithm based on the composite influence of multi-dynamic elements. *Appl. Ocean Res.* 43, 184–194. <https://doi.org/10.1016/j.apor.2013.07.010>.
- Lubkovsky, V., 2009. Determination of Wind-Wave Speed Loss of Vessels for Mixed Type Navigation with Measurement of Wave Parameters by Means of Orthogonally-Linear Wave Meters. Novosibirsk, Russia.
- Maisiuk, Y., Gribkovskaia, I., 2014. Fleet sizing for offshore supply vessels with stochastic sailing and service times. In: *Procedia Computer Science*. Elsevier B.V., pp. 939–948. <https://doi.org/10.1016/j.procs.2014.05.346>.
- Maki, A., Akimoto, Y., Nagata, Y., Kobayashi, S., Kobayashi, E., Shiotani, S., Ohsawa, T., Umeda, N., 2011. A new weather-routing system that accounts for ship stability based on a real-coded genetic algorithm. *J. Mar. Sci. Technol.* 16, 311–322. <https://doi.org/10.1007/s00773-011-0128-z>.
- Mannarini, G., Coppini, G., Oddo, P., Pinardi, N., 2013. A prototype of ship routing decision support system for an operational oceanographic service. *TransNav, Int. J. Mar. Navig. Saf. Sea Transp.* 7, 53–59. <https://doi.org/10.12716/1001.07.01.06>.
- Mannarini, G., Pinardi, N., Coppini, G., Oddo, P., Iafra, A., 2016. VISIR-I: small vessels – least-time nautical routes using wave forecasts. *Geosci. Model Dev. (GMD)* 9, 1597–1625. <https://doi.org/10.5194/gmd-9-1597-2016>.
- Molland, A.F., Turnock, S.R., Hudson, D.A., 2017. Ship Resistance and Propulsion, Ship Resistance and Propulsion. Cambridge University Press. <https://doi.org/10.1017/9781316494196>.
- Nielsen, U.D., 2021. Spatio-temporal variation in sea state parameters along virtual ship route paths. *J. Oper. Oceanogr.* 1–18. <https://doi.org/10.1080/1755876X.2021.1872894>.
- Ruth, E., Thompson, I., 2022. Comparing design assumptions with hindcast wave conditions and measured ship speed and heading. *Ocean Eng.* 247, 110613 <https://doi.org/10.1016/j.oceaneng.2022.110613>.
- Shao, W., Zhou, P., Thong, S.K., 2012. Development of a novel forward dynamic programming method for weather routing. *J. Mar. Sci. Technol.* 17, 239–251. <https://doi.org/10.1007/s00773-011-0152-z>.
- Shin, Y.W., Abebe, M., Noh, Y., Lee, S., Lee, I., Kim, D., Bae, J., Kim, K.C., 2020. Near-optimal weather routing by using improved A* algorithm. *Appl. Sci.* 10 <https://doi.org/10.3390/app1076010>.
- Simonsen, M.H., Larsson, E., Mao, W., Ringsberg, J.W., 2015. State-of-the-Art within Ship Weather Routing. <https://doi.org/10.1115/OMAE2015-41939>.
- Sotillo, Marcos G., Cerralbo, P., Lorente, P., Grifoll, M., Espino, M., Sanchez-Arcilla, A., Alvarez-Fanjul, E., 2020. Coastal ocean forecasting in Spanish ports: the Samoa operational service. *J. Operat. Oceanogr.* 13 (1), 37–54. <https://doi.org/10.1080/1755876X.2019.1606765>.
- Staneva, J., Behrens, A., Ricker, M., Gayer, G., 2020. Black Sea Waves Analysis and Forecast (CMEMS BS-Waves) (Version 2) Set. Copernicus Monitoring Environment Marine Service (CMEMS). https://doi.org/10.25423/CMCC/BLKSEA_ANALYSISFORECAST_WAV_007_003.

- Szlapczynska, J., Smierzchalski, R., 2009. Multicriteria optimisation in weather routing. *TransNav Int. J. Mar. Navig. Saf. Sea Transp.* 3, 393–400.
- Takashima, K., Mezaoui, B., 2009. *TransNav Journal - on the Fuel Saving Operation for Coastal Merchant Ships Using Weather Routing [WWW Document]*.
- Walther, L., Rizvanolli, A., Wendebourg, M., Jahn, C., 2016. Modeling and optimization algorithms in ship weather routing. *Int. J. e-Navigat. Marit. Econ.* 4, 31–45. <https://doi.org/10.1016/j.enavi.2016.06.004>.
- Wang, K., Yan, X., Yuan, Y., Tang, D., 2016. Optimizing ship energy efficiency: application of particle swarm optimization algorithm. *Proc. Inst. Mech. Eng. Part M J. Eng. Marit. Environ.* 232 <https://doi.org/10.1177/1475090216638879>.
- Wu, G., Atilla, I., Tahsin, T., Terziev, M., Wang, L., 2021. Long-voyage route planning method based on multi-scale visibility graph for autonomous ships. *Ocean Eng.* 219, 108242 <https://doi.org/10.1016/j.oceaneng.2020.108242>.
- Zakaria, A., Md Arof, A., Khabir, A., 2022. In: Ismail, A., Dahalan, W.M., Öchsner, A. (Eds.), *Instruments Utilized in Short Sea Shipping Research: A Review BT - Design in Maritime Engineering*. Springer International Publishing, Cham, pp. 83–108.
- Zhao, W., Wang, H., Geng, J., Hu, W., Zhang, Z., Zhang, G., 2022. Multi-objective weather routing algorithm for ships based on hybrid particle swarm optimization. *J. Ocean Univ. China* 21, 28–38. <https://doi.org/10.1007/s11802-022-4709-8>.
- Zis, T., North, R.J., Angeloudis, P., Ochieng, W.Y., Bell, M.G.H., 2014a. Evaluation of cold ironing and speed reduction policies to reduce ship emissions near and at ports. *Marit. Econ. Logist.* 16, 371–398. <https://doi.org/10.1057/mel.2014.6>.
- Zis, T., North, R.J., Angeloudis, P., Ochieng, W.Y., Bell, M.G.H., 2014b. Environmental balance of shipping emissions reduction strategies. *Transport. Res. Rec.* 2479, 25–33. <https://doi.org/10.3141/2479-04>.
- Zis, T.P.V., Psaraftis, H.N., Ding, L., 2020a. Ship weather routing: a taxonomy and survey. *Ocean Eng.* <https://doi.org/10.1016/j.oceaneng.2020.107697>.
- Zis, T.P.V., Psaraftis, H.N., Tillig, F., Ringsberg, J.W., 2020b. Decarbonizing maritime transport: a Ro-Pax case study. *Res. Transp. Bus. Manag.* 37 <https://doi.org/10.1016/j.rtbm.2020.100565>.